Selective Killing of Hypoxia-Inducible Factor-1–Active Cells Improves Survival in a Mouse Model of Invasive and Metastatic Pancreatic Cancer

Shinae Kizaka-Kondoh,[1,2] Satoshi Itasaka,[2] Lihua Zeng,[2,4] Shotaro Tanaka,[2] Tao Zhao,[2,4] Yumi Takahashi,[2] Keiko Shibuya,[2] Kiichi Hirota,[3] Gregg L. Semenza,[5] and Masahiro Hiraoka[2]

Abstract

Purpose: Pancreatic cancer is characterized by intratumoral hypoxia, early and aggressive local invasion, and metastatic potential. Hypoxia-inducible factor-1 (HIF-1) is the major transcriptional activator of hypoxia-responsive genes and intratumoral hypoxia is associated with increased risk of metastasis. However, the behavior of the cells having HIF-1 activity during the malignant progression in pancreatic cancer has not been tested.
Experimental Design: We orthotopically transplanted pancreatic cancer cells stably transfected with a HIF-1–dependent luciferase reporter gene and monitored HIF-1 activity *in vivo* in control and POP33-treated mice. POP33 is a novel prodrug, which has potential to increase caspase-3 activity and induce apoptosis in HIF-1–active/hypoxic cells.
Results: *In vivo* optical imaging showed that HIF-1 activity proceeded along with local invasion, the peritoneal dissemination, and the liver metastasis. HIF-1–active hypoxic cells were selectively eradicated by POP33. Moreover, selective killing of HIF-1–active hypoxic cells significantly suppressed malignant progression, resulting in a significant improvement in survival rate.
Conclusions: These results show that HIF-1–active cells constitute a large proportion of invading and metastatic cells and suggest that eradication of these cells may improve the outcome in advanced pancreatic cancer, a condition for which no effective therapy currently exists.

Pancreatic cancer is one of the most lethal solid tumors of the gastrointestinal tract. The high mortality rate of pancreatic cancer is due to the high incidence of metastatic disease at the time of diagnosis, a fulminant clinical course, and the lack of adequate systemic therapies. Peritoneal and extrapancreatic seeding is observed during end-stage pancreatic cancer. Pancreatic cancer is characterized by extensive invasion into surrounding tissues and metastasis to distant organs, even at an early stage. The prognosis of patients is poor (1) and new systemic agents are urgently needed.

Intratumoral hypoxia is a major factor contributing to cancer progression (1–4). This situation is exacerbated by the high oxygen demands of rapidly proliferating tumor cells, poor lymphatic drainage resulting in high interstitial pressure, and shunting of blood through immature tumor vasculature (3). The evidence for hypoxia in pancreatic cancers includes their characteristic avascular appearance on computed tomography (5) and low intratumoral oxygen tension measurements (6). Furthermore, the expression of target genes of hypoxia-inducible factor-1 (HIF-1), the major transcription factor activated under hypoxic conditions, is elevated in pancreatic cancers (2, 7–11). They include proangiogenic factors such as vascular endothelial growth factor (VEGF), growth/survival factors such as insulin-like growth factor, and extracellular matrix remodeling proteins such as metalloproteinase-9 (12). Thus, HIF-1 activity may play a crucial role in malignant progression of pancreatic cancers.

Orthotopic implantation of human pancreatic cancer cell line SUIT-2 has been reported as a clinically relevant model showing an aggressive and malignant phenotype with liver metastasis, peritoneal dissemination, and ascites (13, 14). Although pathologic studies have shown the progression of pancreatic cancer in this model, the contribution of hypoxic/HIF-1–active tumor cells to the metastatic process has not been evaluated.

Authors' Affiliations: [1]Innovative Techno-Hub for Integrated Medical Bioimaging and [2]Department of Radiation Oncology and Image-applied Therapy, Kyoto University Graduate School of Medicine; [3]Department of Anesthesia, Kyoto University Hospital, Kyoto, Japan; [4]Department of Radiation Medicine, Fourth Military Medical University, Shaanxi, China; and [5]Vascular Program, Institute for Cell Engineering; Departments of Pediatrics, Medicine, Oncology, and Radiation Oncology; and McKusick-Nathans Institute of Genetic Medicine, the Johns Hopkins University School of Medicine, Baltimore, Maryland
Received 9/1/08; revised 2/13/09; accepted 2/14/09; published OnlineFirst 5/5/09.
Grant support: Scientific Research on Priority Areas, Cancer, from the Ministry of Education, Culture, Sports, Science and Technology. This study is a part of joint research, which is focusing on the development of the basis of technology for establishing COE for nanomedicine, carried out through Kyoto City Collaboration of Regional Entities for Advancing Technology Excellence assigned by Japan Science and Technology Agency.
The costs of publication of this article were defrayed in part by the payment of page charges. This article must therefore be hereby marked *advertisement* in accordance with 18 U.S.C. Section 1734 solely to indicate this fact.
Requests for reprints: Shinae Kizaka-Kondoh, Department of Radiation Oncology and Image-applied Therapy, Kyoto University Graduate School of Medicine, 54 Shogoin-Kawahara-cho, Sakyo-ku, Kyoto 606-8507, Japan. Phone: 81-75-751-4242; Fax: 81-75-771-9749; E-mail: skondoh@kuhp.kyoto-u.ac.jp.

doi:10.1158/1078-0432.CCR-08-2267

Translational Relevance

Advanced pancreatic cancer exhibits a high mortality rate, and currently, no effective therapy exists for it. Our findings may encourage the development of novel strategies and drugs to target hypoxia-inducible factor-1 (HIF-1)–active cells in advanced pancreatic cancer. One such strategy we have developed is the prodrug POP33, which selectively induces apoptosis of HIF-1–active/hypoxic cells. POP33 significantly suppresses the malignant progression of advanced pancreatic cancer in animal experiments. Combination therapy of this HIF-1–targeting strategy with chemotherapy may open a new avenue to improve outcome in advanced pancreatic cancer.

HIF-1 is a transcription factor composed of HIF-1α and HIF-1β subunits. Under normoxic conditions, HIF-1α protein is degraded by ubiquitination and proteasomal degradation following hydroxylation of proline residues in the oxygen-dependent degradation (ODD) domain (15). Under hypoxic conditions, HIF-1α protein accumulates and translocates to the nucleus where it heterodimerizes with HIF-1β to form an active transcription factor. More than 60 putative direct HIF-1 target genes have been identified and many of them are implicated in angiogenesis, invasion, and metastasis (12). Furthermore, HIF-1 has been recognized as a major resistance factor for anticancer therapies such as chemotherapy (16–19) and radiotherapy (20–22). Thus, HIF-1 activity is a hallmark of tumor malignancy.

We hypothesized, first, that the invasion and metastasis of pancreatic cancer is associated with hypoxia and increased HIF-1 activity and, second, that therapy targeting HIF-1–active cells would impair malignant progression. We developed and validated a fusion protein, TAT-ODD-procaspase-3 (TOP3), to specifically eradicate HIF-1–active hypoxic cells (20, 23–28). TOP3 consists of three domains. The TAT protein transduction domain (PTD) efficiently delivers the fusion protein into cells *in vivo* (29). The ODD domain contains a VHL-mediated protein destruction motif from the human HIF-1α protein that confers hypoxia-dependent stabilization to the fusion protein (25). The procaspase-3 domain is an inactive proenzyme form of human caspase-3 that is activated by preexisting apoptotic signals in hypoxic cells.

Here, we report a newly developed fusion protein, POP33, which has a novel PTD that mediates significantly higher protein transduction activity than TAT-PTD. We examined the activity of PP33 in a clinically relevant orthotopic model of pancreatic cancer. We serially monitored HIF-1–active cancer cells with a bioluminescence photon counting device and showed their involvement in local invasion and metastasis. POP33 significantly increased caspase-3 activity, suppressed peritoneal dissemination, and prolonged survival. These results indicate that HIF-1 activity plays a crucial role in malignant progression and support the use of drugs targeting HIF-1 for the treatment of pancreatic cancer.

Materials and Methods

Cell culture and isolation of SUIT-2/EF-Luc and SUIT-2/HRE-Luc cells. The human pancreatic cancer cell line SUIT-2 was purchased from the American Type Culture Collection. SUIT-2/EF-Luc and SUIT-2/HRE-Luc

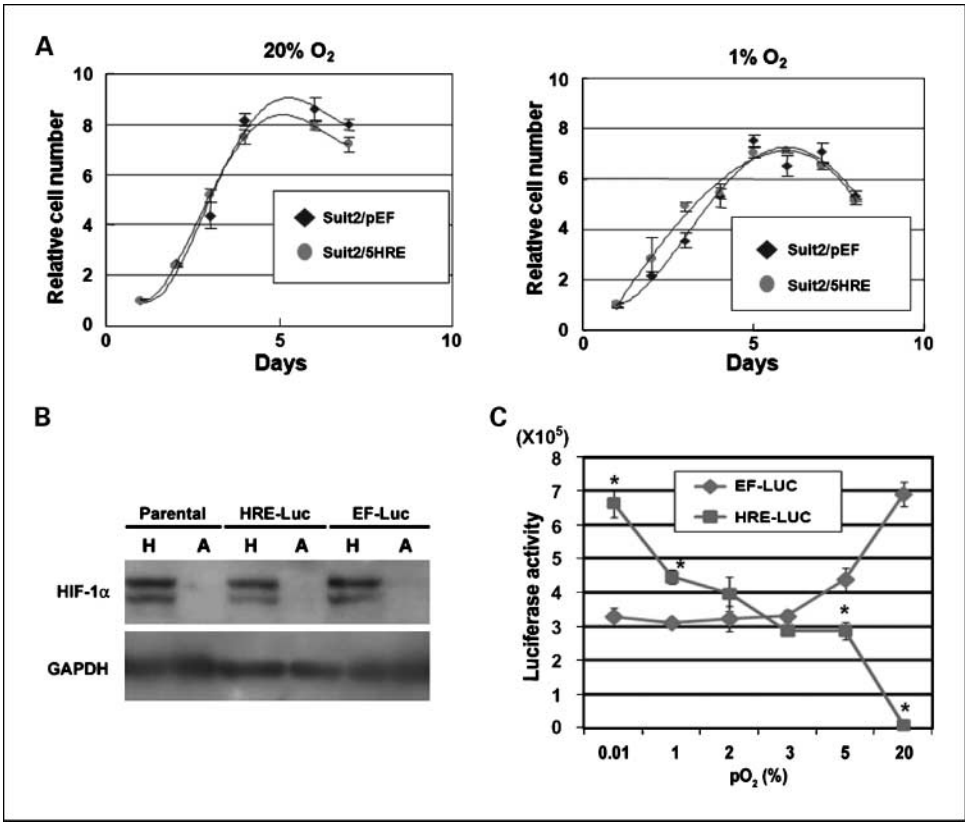

Fig. 1. Characterization of SUIT-2 cell lines with luciferase reporter genes. *A,* SUIT-2/EF-Luc and SUIT-2/HRE-Luc cells were cultured for the indicated time under aerobic (20% O_2) and hypoxic (1% O_2) conditions. At the end of the culture period, cells were counted and mean cell number relative to day1 is shown. *B,* SUIT-2/EF-Luc, SUIT-2/HRE-Luc, and their parental SUIT-2 cells (*Parental*) were cultured for 20 h under aerobic (*A*) and hypoxic (*H*) conditions. Total cell lysate (30 μg) was analyzed for HIF-1α and glyceraldehyde-3-phosphate dehydrogenase (*GAPDH*; as an internal control) expression by Western blotting. *C,* SUIT-2/EF-Luc and SUIT-2/HRE-Luc cells were cultured in a 5% CO_2 incubator at the indicated O_2 concentration for 18 h. Then, luciferase activity of each cell lysate preparation was measured. Points, mean ($n = 5$); bars, SE. *, $P < 0.05$.

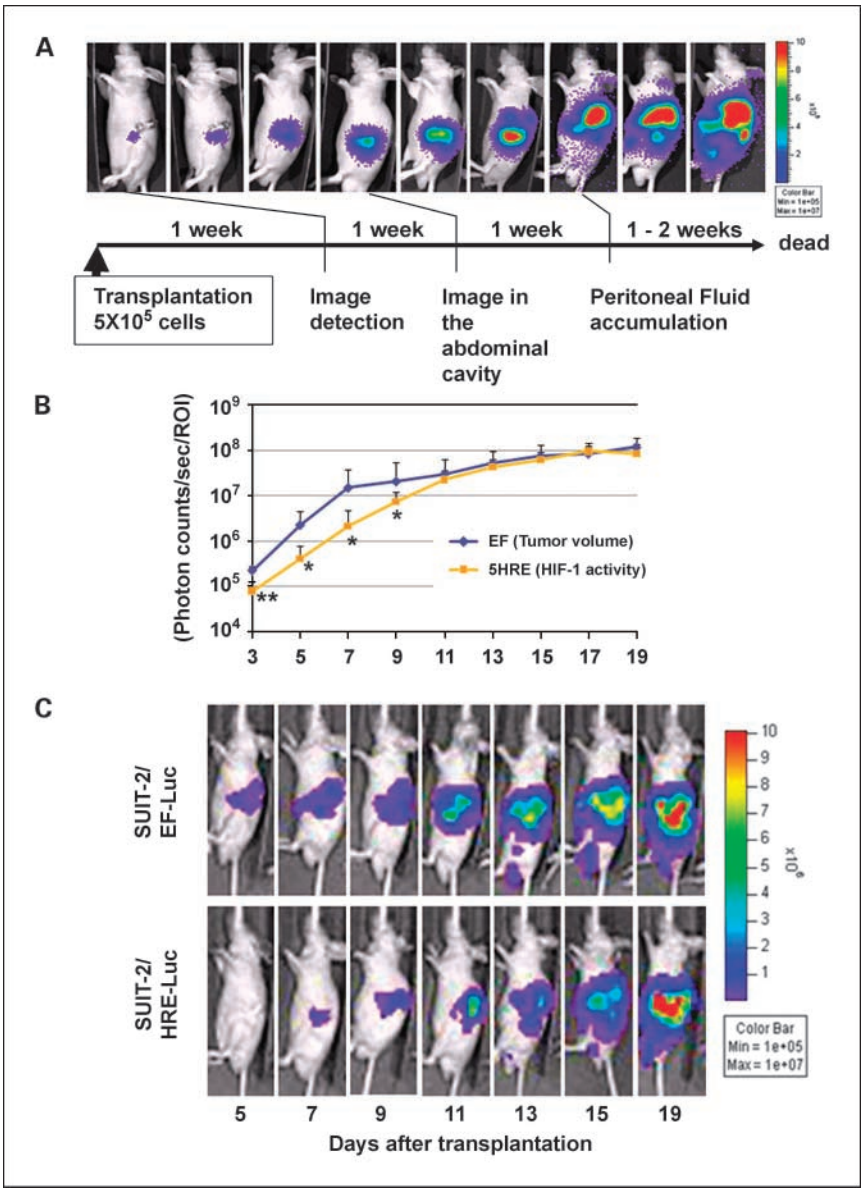

Fig. 2. Images of tumor mass and HIF-1 activity in an orthotopic model of pancreatic cancer. *A,* typical HIF-1 image during pancreatic cancer progression. SUIT-2/HRE-Luc cells (5×10^5) were transplanted into the pancreas. Approximately 1 wk after transplantation, significant bioluminescence ($>1 \times 10^5$ photon counts/s/ROI) was detected at the transplant site. During the next week, the signal increased, and by the 3rd week, the signal spread to the abdominal cavity. By the 4th week, ascites accumulated. Approximately 5 to 6 wk after transplantation, the mice died with fulminant ascites. *B,* nude mice ($n = 5$ in each group) were orthotopically transplanted with 5×10^5 SUIT-2/EF-Luc (*left graph*) or SUIT-2/HRE-Luc (*right graph*) cells. Bioluminescence intensity was monitored every other day between 3 and 19 d after orthotopic transplantation. *, $P < 0.5$; **, $P < 0.05$. *C,* representative images of *B*. Images of the mice orthotopically transplanted with SUIT-2/EF-Luc (*top*) and SUIT-2/HRE-Luc (*bottom*) between day 5 and day 19 after orthotopic transplantation are shown.

cells were isolated from a colony formed after transfection with plasmid pEF/Luc and pEF/HRE-Luc, respectively (24), by calcium phosphate method (30) and antibiotic selection. The cells were maintained at 37°C in 5% FCS-DMEM (Nacalai Tesque) supplemented with penicillin (100 units/mL) and streptomycin (100 μg/mL). Hypoxic cell cultures were done in 5% CO_2-1% O_2 in a multigas incubator (ASTEC).

Growth assay. SUIT-2/EF-Luc and SUIT-2/HRE-Luc cells (100/100 μL/well) were seeded in a 96-well plate and cultured at 20% or 1% O_2. The following day, 5 μL of SF cell counting reagent containing 2-(2-methoxy-4-nitrophenyl)-3-(4-nitrophenyl)-5-(2, 4-disulfophenyl)-2H-tetrazolium, monosodium salt (Nacalai Tesque) were added to each well, and 24 h later, the plates were monitored by a plate reader photometer (absorbance at 450 nm). The assay was repeated every day. The absorbance of each well was divided by the absorbance on day 1 to calculate the relative cell number. The experiments were done in triplicate and results were presented as mean relative absorbance ± SE. The experiment was repeated thrice.

Luciferase activity assay. Cells (10^4) were seeded onto 24-well plate and cultured overnight and then further cultured in an ordinary CO_2 incubator or a hypoxic chamber BACLITE-1 (pO_2, >0.02%; Sheldon Manufacturing) for 18 h. The cells were lysed and their luciferase activity was measured as described previously (19).

Western blot analysis. SUIT-2/EF-Luc, SUIT-2/HRE-Luc, and parental SUIT-2 cells were cultured under hypoxic (1% O_2) or aerobic (20% O_2) conditions for 20 h and then cells were harvested and the cell lysates were analyzed by Western blotting as described previously (19). The experiment was repeated thrice.

***Orthotopic transplantation of tumor cells and real-time monitoring of luciferase activity* in vivo.** Orthotopic transplantation of tumor cells was done as described previously (31). Briefly, SUIT-2/HRE-Luc or SUIT-2/EF-Luc cells (1×10^5/25 μL) mixed with an equal volume of Geltrex (Invitrogen) were injected into the pancreas of 8-wk-old male nude mice (BALB/c-*nu/nu*; Japan SLC, Inc.). For the *in vivo* photon counting of bioluminescence, tumor-bearing mice were i.p. injected with 200 μL of D-luciferin solution (10 mg/mL in PBS; Promega Corp.). Acquisition and analysis of images were done with IVIS-200 (Xenogen Corp.) as described previously (24). As background photon counts/second in untreated nude mice (with D-luciferin injection) were <4,000, we considered $>1 \times 10^4$ photon counts/s a significant signal and

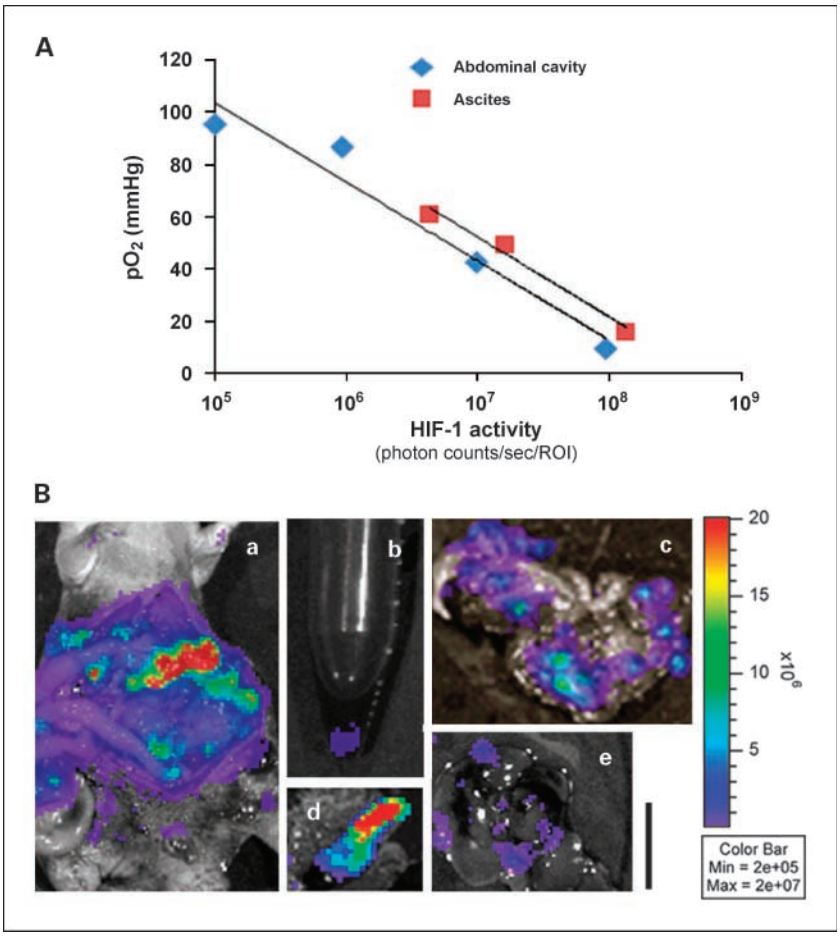

Fig. 3. pO_2 and HIF-1 activity during cancer progression. *A,* the values of pO_2 (mm Hg) in the abdominal cavity (*blue diamond*) and the ascites (*orange square*) and bioluminescence intensity corresponding to HIF-1 activity (photon counts/second/ROI) in the mice are shown. *B,* when a mouse orthotopically transplanted with SUIT-2/HRE-Luc cells developed ascites (23 d after tumor cell implantation), it was injected with D-luciferin, and 13 min later, the mouse was dissected. Then, the ascites fluid was collected in a centrifuge tube. HIF-1–active tumor cells in the opened abdomen (*a*), the ascites fluid (*b*), the intestines (*c*), the pancreas (*d*), and the liver (*e*) were imaged. The images were taken by 20 min after D-luciferin injection. Bar, 10 mm.

showed images >1 × 10^5 photon counts/s in the figures. The minimum and maximum photons/second of each figure are indicated in each rainbow bar scale.

Measurement of pO_2 in the abdominal cavity. Mice were anesthetized by 2.5% of isoflurane gas in oxygen flow (25 mL/s) and kept on a heating pad to maintain body temperature between 37°C and 38°C. A needle (20 G × $1^{1/2}$, TERUMO) was inserted and fixed on the abdominal skin with a quick-drying glue. A modified $PtiO_2$ probe (LICOX CC1.R, 7-mm sensitive area length, 0.65-mm diameter; Integra NeuroSciences) was inserted into the abdominal cavity through the needle and connected to the LICOX CMP instrument (Integra NeuroSciences). The most outer code cover was fixed to the needle with a quick-drying glue so that the abdominal cavity was kept closed. The oxygen partial pressure was measured for >5 min and automatically recorded every 20 s while a needle-type electrode was moved throughout the abdominal cavity. The average oxygen concentration (mm Hg) ± SE was calculated from each record. Ascites samples were drawn from the abdominal cavity by puncturing with heparin-containing syringes and then immediately subjected to analysis (ABL 700 series, Radiometer) for oxygen tension.

ELISA assay for VEGF. Ascites fluid collected from the mice was left to stand at room temperature for 2 h and then centrifuged for 20 min at 2,000 × *g*. The supernatant was immediately assayed for VEGF concentration with the Quantikine mouse VEGF immunoassay kit (R&D Systems).

Preparation and analysis of recombinant EGFP proteins. Expression vector plasmids of PTD-EGFP fusion proteins encoding enhanced green florescent protein were constructed by inserting the cDNA fragments encoding PTD, which was prepared by annealing corresponding oligonucleotides, and EGFP, which was excised from pEF-EGFP (Promega), into plasmid pGEX-6P-3. Recombinant proteins were prepared as described previously (20) and suspended in PBS at a final concentration of 50 μmol/L. The cells were trypsinized and suspended in 300 μL of ice-cold PBS. The fluorescence intensity of the cells was determined by fluorescence-activated cell sorting using CellQuest (Becton Dickinson).

POP33 preparation and administration to mice. DNA sequences encoding PTD3 were prepared by annealing appropriate oligonucleotides and replaced the TAT-ptd sequence present in TOP3. POP33 fusion protein was prepared as described previously for TOP3 (23). POP33 suspended in 10 mmol/L Tris buffer (1 mg/mL) was i.p. injected into tumor-bearing mice (5 mg/kg).

In vivo *imaging of caspase-3 activity.* For preparation of Z-DEVD-aminoluciferin, 10 mg of VivoGlo Caspase-3/7 substrate (Promega) were dissolved in 67 μL of surfactant mix (70 μL of Tween 80, 640 μL of PEG 400, and 290 μL of *N,N*-dimethylacetamide) and then added to 100 μL of 5% dextrose in water. The mixture was vortexed to make a homogenous solution and peritoneally injected into tumor-bearing mice (100 μL/mouse). Ten minutes after Z-DEVD-aminoluciferin injection, the mice were imaged with IVIS.

Statistical analysis. The Kaplan-Meier method was used to determine survival curves, and comparisons between the curves were done by log-rank test. The statistical analyses were done using Statistical Package for the Social Sciences 16.0 for Windows and Excel. A P value of <0.05 was considered statistically significant.

Results

Characterization of SUIT-2 pancreatic cancer cells with luciferase reporter genes. HIF-1α overexpression is one of the hallmarks of malignancy (32). We hypothesized that HIF-1–activity represents

an important driving force for invasion and metastasis. To test this hypothesis, we did serial quantitative measurements of HIF-1 activity in xenografts derived from cancer cell lines stably transfected with plasmid p5HRE-luciferase (21), which expressed firefly luciferase under the control of a HIF-1–dependent promoter. We applied this system to a clinically relevant orthotopic model to determine the levels of HIF-1 activity during the progression of pancreatic cancer. We first established a stable human pancreatic cancer cell line, SUIT-2/HRE-Luc. The control cell line SUIT-2/EF-Luc constitutively expressed luciferase, and thus, the luciferase activity was proportional to the tumor mass (21). The growth (Fig. 1A) and HIF-1α expression (Fig. 1B) of these cell lines were similar. The luciferase activity in SUIT-2/HRE-Luc cells under hypoxic conditions was >100 times higher than under aerobic conditions (Fig. 1C). Conversely, the luciferase activity in SUIT-2/EF-Luc decreased as pO_2 decreased (Fig. 1C), reflecting the global inhibition of transcription and translation that occurs in response to hypoxia (33).

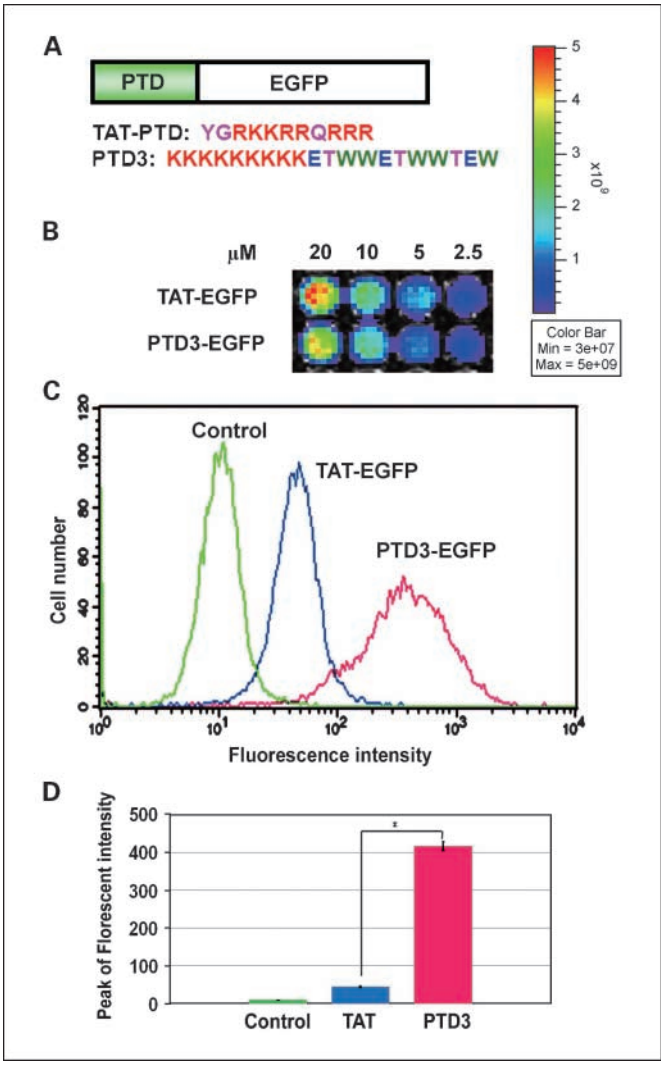

Fig. 4. Protein transduction activity of PTD3. *A,* the amino acid sequences of TAT-ptd and PTD3 are shown. Amino acids are color coded based on their chemical properties: green, hydrophobic; red, basic; blue, acidic; pink, hydrophilic or uncharged polar. *B,* the fluorescent intensity of 50 μL TAT-ptd-EGFP and PTD-EGFP at the indicated concentration was measured by IVIS (λ-excitation, 445-490 nm; λ-emission, 515-575 nm). The photon counts/second/ROI of TAT-ptd-EGFP and PTD-EGFP were the following: 20 μmol/L, 1.86×10^{10} and 1.51×10^{10}; 10 μmol/L, 9.50×10^{9} and 8.14×10^{9}; 5 μmol/L, 5.33×10^{9} and 4.04×10^{9}; 2 μmol/L, 1.70×10^{9} and 1.49×10^{9}, respectively. *C* and *D,* fusion protein (25 μL of 50 μmol/L preparation) was added to the cells and incubated for 30 min. The cells were trypsinized and their fluorescence intensity was measured by flow cytometry. *C,* representative fluorescence-activated cell sorting data. *D,* the experiments were done in triplicate and peak of fluorescence intensity is shown. Columns, mean; bars, SE. *, $P < 0.001$. Three independent experiments of *C* and *D* were done, and basically, the same results were obtained.

In vivo *imaging of the progression of pancreatic cancer.* The orthotopic model using SUIT-2 cells has been extensively studied and well characterized (13). SUIT-2 cells, which are c-Met positive, form invasive tumors with peritoneal dissemination and fulminant ascites in a reproducible manner (13). We transplanted SUIT-2/EF-Luc and SUIT-2/HRE-Luc cells to the pancreas and measured the intensity of the bioluminescent signal [photons/second/region of interest (ROI)]. The bioluminescent signals from SUIT-2/EF-Luc and SUIT-2/HRE-Luc xenografts reflect tumor mass and HIF-1 activity, respectively.

A preliminary experiment was done with mice bearing various size of xenografts and found that the photon counts of all xenografts peaked between 13 and 15 minutes after D-luciferin injection (Supplementary Fig. S1) Thus, in the subsequent experiments, we acquired images of the transplanted mice between 13 and 15 minutes after D-luciferin injection.

Representative bioluminescence images of HIF-1 activity during progression of the orthotopic pancreatic tumor model are shown in Fig. 2A. A significant signal over background was detected at the injection site 1 to 2 weeks after orthotopic transplantation; by the following week, it had spread to the abdomen; by the 3rd week, it had spread throughout the abdomen with peritoneal fluid accumulation; and by 4 weeks after initial signal detection, 100% of mice had died with massive ascites. Although the time course of the increases in tumor mass (SUIT-2/EF-Luc) and HIF-1 activity (SUIT-2/HRE-Luc) was similar, increases in HIF-1 activity were delayed about a week compared with increases in tumor mass (Fig. 2B and C), suggesting that the HIF-1 activity corresponded to the development of hypoxic regions in the growing cancers. Interestingly, the timing of increased bioluminescence associated with spread of cancer to the abdominal cavity, typically 11 to 13 days after transplantation, was the same for the tumor mass and HIF-1 activity (Fig. 2C), indicating that the tumor cells invading the abdominal cavity already had HIF-1 activity.

Peritoneal dissemination caused hypoxia in the abdominal cavity. To directly measure pO_2 in the abdominal cavity at different stages of tumor progression, a $PtiO_2$ probe was inserted into the abdominal cavity. Real-time monitoring of pO_2 throughout the abdominal cavity was done over 5 minutes. When tumor cells were localized to the transplant site and no ascites was detected (Fig. 3A, *left*), pO_2 in the abdomen was 86.4 ± 10.1 mm Hg, which was similar to the oxygen concentration in untreated mice (98.5 ± 9.5 mm Hg). On the other hand, when HIF-1–specific bioluminescence spread to the abdomen (~5×10^{6} photon counts/s/ROI), the pO_2 was significantly decreased (42.5 ± 5.6 mm Hg). When the abdominal cavity was filled with ascites and a strong signal (~1×10^{8} photon counts/s/ROI) was detected throughout the abdomen, pO_2 was <10 mm Hg. Ascites fluid accumulated significantly when the HIF-1–specific bioluminescent signal was >1×10^{7} photon counts/s/ROI. The pO_2 of ascites was also measured and was similar to the abdominal cavity (Fig. 3A). HIF-1 activity was reciprocally correlated

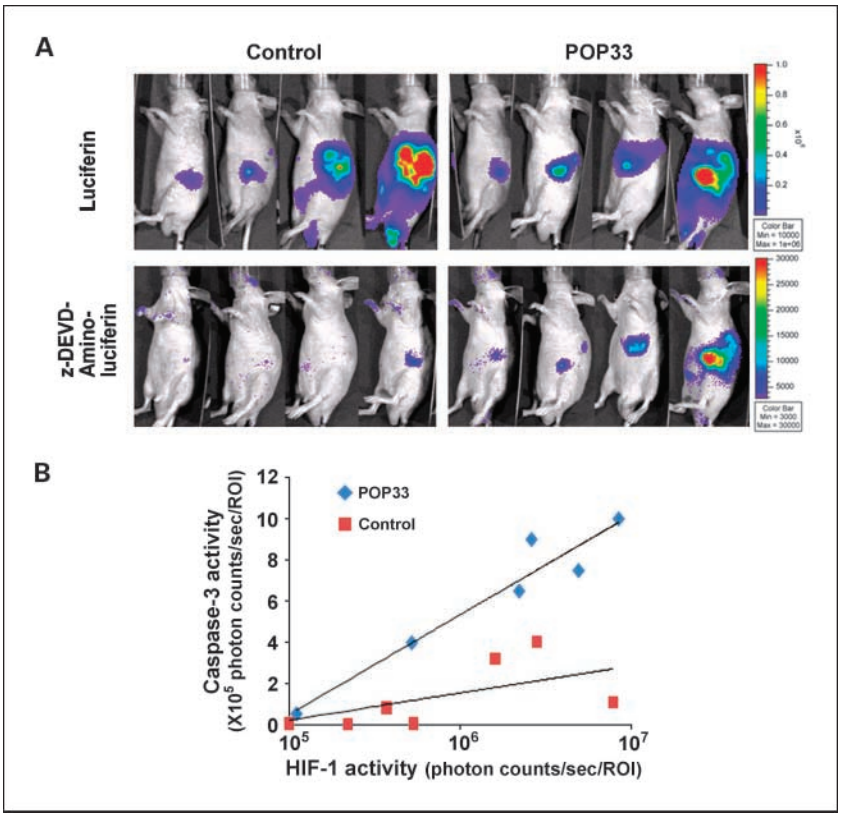

Fig. 5. Increased caspase-3 activity in xenografts after POP33 treatment. *A*, top, mice orthotopically transplanted with SUIT-2/HRE-Luc cells at various stages of progression were divided into two groups, control and POP33, according to the images after D-luciferin injection. Mice in the control group were injected with buffer alone and mice in the POP33-treated group were injected with 5 mg/kg POP33. Bottom, 6 h later, the mice were injected with a caspase-3–specific prosubstrate, Z-DEVD-aminoluciferin, and 10 min later, bioluminescence was measured. *B*, bioluminescence intensity (photon counts/second/ROI) after D-luciferin (*Y axis*) and Z-DEVD-aminoluciferin (*X axis*) injection of control mice (*orange square*) and POP33-treated mice (*blue diamond*). Pearson's correlation is significant at the 0.01 level (two tailed).

with oxygen tension in both the abdominal cavity and ascites (Fig. 3A).

At the final stage of the pancreatic cancer, the ascites contained extremely high levels (between 1,000 and 2,200 pg/mL) of VEGF, a prototypical HIF-1 target gene product. The serum levels of VEGF in control mice were 113.2 ± 30.8 pg/mL. These results confirm that hypoxia induces HIF-1 activity in this model. Together with Fig. 2, these results suggest that HIF-1–active cancer cells invade locally and create hypoxic conditions during growth and dissemination throughout the abdominal cavity.

Pancreatic cancer cells with HIF-1 activity were also visualized by bioluminescent imaging postmortem. Mice with fulminant ascites were dissected 13 minutes after D-luciferin injection and HIF-1 activity of xenografts in the abdominal cavity was directly examined by *ex vivo* imaging (Fig. 3B, *a-e*). The average volume of ascites was 4.1 mL when mice died with fulminant ascites. Cells in the ascites, which were collected by centrifugation, also had high levels of luciferase activity (Fig. 3B, *b*). Bioluminescence was also detected in the intestines (Fig. 3B, *a* and *c*), primary tumors in the pancreas (Fig. 3B, *d*), and liver metastases (Fig. 3B, *e*). These data indicate that HIF-1–active tumor cells contribute to local invasion, metastasis, and peritoneal dissemination.

Construction of a novel hypoxia-targeting protein drug. We hypothesized that if HIF-1–active cells play a crucial role during the progression of pancreatic cancer, eradication of these cells would suppress invasion and metastasis. For eradication of HIF-1–active cells, we previously developed and validated a hypoxia-targeting prodrug, TOP3, which efficiently induced apoptosis and decreased HIF-1 activity in tumors (23, 24) and significantly enhanced radiotherapy (20). To improve efficacy, we constructed POP33, which contains a novel protein transduction domain, PTD3, consisting of polylysine and noncharged amino acids (Fig. 4A). To assess the membrane transduction function of PTD fusion proteins, PTD3 (present in POP33) and TAT-ptd (present in TOP3) were fused to EGFP and their membrane transduction activity was assessed with a fluorescence microscopy and flow cytometry. The fusion proteins had similar fluorescent intensity *in vitro* (Fig. 4B). SUIT-2/HRE-Luc cells were treated with PTD3-EGFP or TAT-ptd-EGFP for 30 minutes and washed extensively. The cells were then trypsinized and their fluorescent intensity was quantified by flow cytometry (Fig. 4C). The results indicate that PTD3 has more than five times higher cell-penetrating activity than TAT-PTD.

In vivo *caspase-3 activity induced by POP33 treatment.* Apoptosis induction by TOP3 was previously observed *in vitro* (23, 25) and in tumor sections by terminal deoxynucleotidyl transferase–mediated dUTP nick end labeling (24). To directly examine the ability of POP33 to increase caspase-3 activity *in vivo*, we used Z-DEVD-aminoluciferin (34), a prosubstrate that is converted to a luciferase substrate when cleaved by caspase-3. POP33 or buffer alone was i.p. injected into mice with various degrees of HIF-1–dependent bioluminescence (Fig. 5A, *top*). Six hours later, Z-DEVD-aminoluciferin was injected and caspase-3 activity was determined (Fig. 5A, *bottom*). Caspase-3 activity increased as HIF-1 activity increased in both control and POP33-treated mice [Fig. 5A (*top*) and B]. However, in the POP33-treated mice, higher caspase-3–dependent bioluminescence was detected compared with control mice with similar levels of HIF-1–dependent bioluminescence (Fig. 5B). These

results indicate that the procaspase-3 domain in POP33 is cleaved, thereby increasing caspase-3 activity in HIF-1–active/hypoxic tumor cells.

POP33 suppressed peritoneal dissemination and improved survival. When total photon counts were ~1 × 10^5 photons/s/ROI, mice were randomized to control and treatment groups. Representative *ex vivo* images of tumors with 1 × 10^5 and 1 × 10^6 photons/s/ROI are shown in Supplementary Fig. S2. The mice in the treatment group (n = 8) were injected with 5 mg/kg POP33 every 4 days until the mouse expired or was euthanized. We treated the mice in this way because PTD-ODD-procaspase-3 does not affect well-oxygenized proliferating tumor cells, and thus, growing tumors make new hypoxic fractions and increase HIF-1 activity in the tumors 3 days after the treatment (20, 23, 24). HIF-1 activity in the xenografts of untreated mice rapidly increased, and all of the mice died by 24 days after the initial image detection [Fig. 6A (*left graph*) and B (*top*)]. On the other hand, in half of the mice treated with POP33, HIF-1 activity in the xenografts increased more slowly or stayed at low levels [Fig. 6A (*right graph*) and B (*bottom*)]. The survival of the POP33-treated mice was significantly extended ($P < 0.05$, log-rank analysis). The median survival time of the treated mice was 23 days compared with 13 days for untreated mice (Fig. 6C).

Discussion

HIF-1α expression has been shown in the majority of human cancers, and there is a direct correlation between the degree of overexpression and patient mortality in many types of

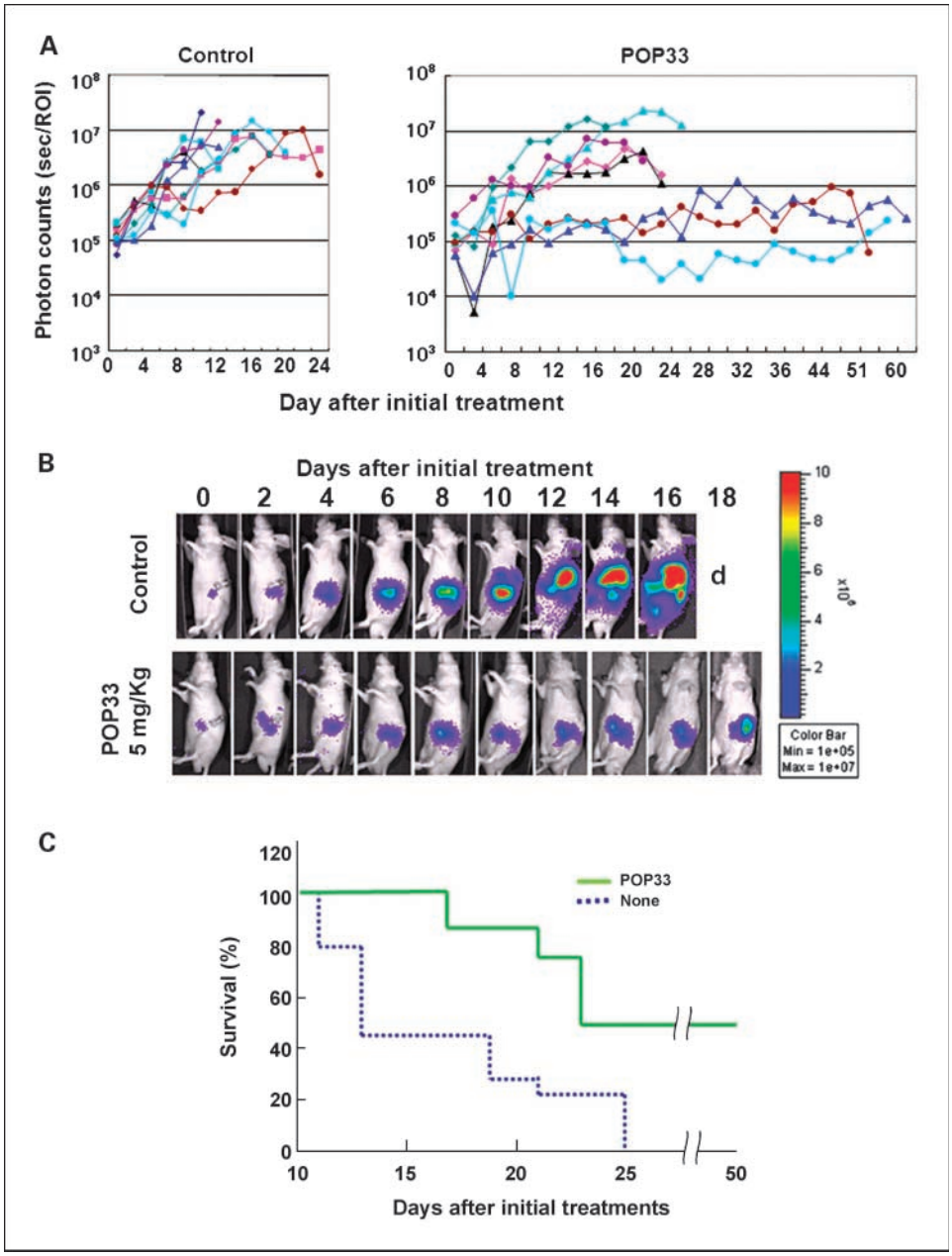

Fig. 6. POP33 suppressed the progression of pancreatic cancer. *A,* mice (n = 8) were treated with buffer alone (control) or POP33 (5 mg/kg) every 4th day. The treatments were started (on day 0) when the photon counts of local signal (second/ROI) became ~1 × 10^5. Serial images were acquired every other day until day 62 and bioluminescence intensity (photon counts/second/ROI) of image is recorded on the graph. *B,* representative images from the experiment described in *A. C,* Kaplan-Meier survival curves for the experiment presented in *A.*

cancer (12, 32). In the current study, we visualized HIF-1 activity in an orthotopic pancreatic cancer model using the HIF-1–dependent expression of luciferase and *in vivo* bioluminescent imaging and showed a strong correlation between HIF-1 activity and tumor progression. These results are consistent with the hypothesis that "HIF-1 activity plays a crucial role in invasion and metastasis." In this model, 100% of mice died with peritoneal dissemination and fulminant ascites. The abdominal cavity filled with ascites was severely hypoxic (<10 mm Hg) at the terminal stage. This result was consistent with the observation that the level of VEGF, which is a prototypical HIF-1 target gene product (35), was dramatically increased in ascites, as previously described for human pancreatic cancer specimens (36).

The bioluminescent signal in SUIT-2/EF-Luc–transplanted mice corresponded to the previously reported progression of SUIT-2 pancreatic cancer model (13). The appearance of the bioluminescent signal from SUIT-2/HRE-Luc xenografts (HIF-1 activity) was significantly delayed about a week compared with the constitutive signal from SUIT-2/EF-Luc xenografts (tumor mass). Because the growth rates of both cell lines were comparable *in vitro*, it is likely that both cell lines grow at similar rates *in vivo* and that the signal from SUIT-2/HRE xenografts reflects tumor hypoxia. Therefore, a hypoxic microenvironment must have developed about a week after a tumor mass formed at the transplant site. Furthermore, the images of HIF-1 activity and tumor mass (from day 13) appeared almost identical between these two cell lines, indicating that HIF-1–active/hypoxic cells were the major population during cancer progression. HIF-1 imaging showed the process of pancreatic cancer progression from local growth in the pancreas to invasion of the abdominal cavity and then peritoneal dissemination, which was associated with severe hypoxia. Taken together, these results indicate that HIF-1–active cancer cells play an important role in the malignant progression of pancreatic cancers.

The abdominal cavity was not hypoxic (pO_2, ~85 mm Hg) in non–tumor-bearing mice. However, when HIF-1–active cells invaded the abdominal cavity, the local pO_2 decreased as the HIF-1 activity increased. Taken together with the bioluminescence imaging data, these results suggest that HIF-1–active cancer cells locally invaded, proliferated, and disseminated, creating a severely hypoxic environment.

Based on these findings, we have pursued strategies to target hypoxic pancreatic cancer cells. PTD-ODD-procaspase-3 fusion proteins must enter cells to induce apoptosis, and thus, PTD function is very important for their efficacy. To improve PTD function, we constructed PTD3, which consists of two polar amino acid sequences, a hydrophobic tryptophan-rich motif related to Pep-1 (37), and polylysine. PTD3 endowed the fusion protein with higher membrane-penetrating activity than TAT-PTD sequences. The precise mechanism of PTD3 membrane penetration is under investigation.

The significance of HIF-1 in pancreatic cancer has been suggested (8–11, 38). HIF-1–targeting prodrug POP33 successfully suppressed local invasion and thus peritoneal dissemination. Hypoxia activates caspase-3 in cells to some extent *in vivo* as well as *in vitro* (23–25). Here, we directly showed that it is also true *in vivo* by visualization of caspase-3 activity with a real-time imaging method; in untreated mice, cancer cells had some caspase-3 activity, which also increased as HIF-1 activity increased. PTD-ODD-procaspase-3 increased the caspase-3 activity significantly higher than the control (23–25) and enhanced apoptosis *in vivo* (23, 25), suppressing the tumor growth (24), metastasis (26), and local invasion of HIF-1–active cell in the pancreatic cancer. These results not only show that HIF-1 plays a crucial role in the progression of cancers but also suggest that eradication of HIF-1–active cells may improve the therapeutic outcome in pancreatic cancer.

Disclosure of Potential Conflicts of Interest

No potential conflicts of interest were disclosed.

Acknowledgments

We thank Dr. Ohtsura Niwa (National Institute of Radiological Sciences) for discussion, Waka Kawaguchi for skilled technical assistance, Shigeaki Watanabe (Summit Pharmaceuticals International Corp.) for discussion and technical support of IVIS, and Tadaki Kido (Medical Agent Corp.) for $PtiO_2$ probe (LICOX CC1.R) operation.

References

1. Brahimi-Horn MC, Chiche J, Pouysségur J. Hypoxia and cancer. J Mol Med 2007;85:1301–7.
2. Duffy JP, Eibl G, Reber HA, Hines OJ. Influence of hypoxia and neoangiogenesis on the growth of pancreatic cancer. Mol Cancer 2003;2:12.
3. Giatromanolaki A, Harris AL. Tumor hypoxia, hypoxia signaling pathways and hypoxia inducible factor expression in human cancer. Anticancer Res 2001;21:4317–24.
4. Vaupel P, Mayer A. Hypoxia in cancer: significance and impact on clinical outcome. Cancer Metastasis Rev 2007;26:225–39.
5. Megibow AJ. Pancreatic adenocarcinoma: designing the examination to evaluate the clinical questions. Radiology 1992;183:297–303.
6. Koong AC, Mehta VK, Le QT, et al. Pancreatic tumors show high levels of hypoxia. Int J Radiat Oncol Biol Phys 2000;48:919–22.
7. Garcea G, Doucas H, Steward WP, Dennison AR, Berry DP. Hypoxia and angiogenesis in pancreatic cancer. ANZ J Surg 2006;76:830–42.
8. Akakura N, Kobayashi M, Horiuchi I, et al. Constitutive expression of hypoxia-inducible factor-1α renders pancreatic cancer cells resistant to apoptosis induced by hypoxia and nutrient deprivation. Cancer Res 2001;61:6548–54.
9. Kitada T, Seki S, Sakaguchi H, Sawada T, Hirakawa K, Wakasa K. Clinicopathological significance of hypoxia-inducible factor-1α expression in human pancreatic carcinoma. Histopathology 2003;43:550–5.
10. Shibaji T, Nagao M, Ikeda N, et al. Prognostic significance of HIF-1α overexpression in human pancreatic cancer. Anticancer Res 2003;23:4721–7.
11. Kitajima Y, Ide T, Ohtsuka T, Miyazaki K. Induction of hepatocyte growth factor activator gene expression under hypoxia activates the hepatocyte growth factor/c-Met system via hypoxia inducible factor-1 in pancreatic cancer. Cancer Sci 2008;99:1341–7.
12. Semenza GL. Targeting HIF-1 for cancer therapy. Nat Rev Cancer 2003;3:721–32.
13. Tomioka D, Maehara N, Kuba K, et al. Inhibition of growth, invasion, and metastasis of human pancreatic carcinoma cells by NK4 in an orthotopic mouse model. Cancer Res 2001;61:7518–24.
14. Shono M, Sato N, Mizumoto K, et al. Stepwise progression of centrosome defects associated with local tumor growth and metastatic process of human pancreatic carcinoma cells transplanted orthotopically into nude mice. Lab Invest 2001;81:945–52.
15. Kaelin WG, Jr., Ratcliffe PJ. Oxygen sensing by metazoans: the central role of the HIF hydroxylase pathway. Mol Cell 2008;30:393–402.
16. Liu L, Ning X, Sun L, et al. Hypoxia-inducible factor-1α contributes to hypoxia-induced chemoresistance in gastric cancer. Cancer Sci 2008;99:121–8.
17. Brown LM, Cowen RL, Debray C, et al. Reversing hypoxic cell chemoresistance *in vitro* using genetic and small molecule approaches targeting hypoxia inducible factor-1. Mol Pharmacol 2006;69:411–8.
18. Unruh A, Ressel A, Mohamed HG, et al. The hypoxia-inducible factor-1α is a negative factor for tumor therapy. Oncogene 2003;22:3213–20.
19. Zeng L, Kizaka-Kondoh S, Itasaka S, et al.

Hypoxia inducible factor-1 influences sensitivity to paclitaxel of human lung cancer cell lines under normoxic conditions. Cancer Sci 2007;98:1394–401.

20. Harada H, Kizaka-Kondoh S, Li G, et al. Significance of HIF-1-active cells in angiogenesis and radioresistance. Oncogene 2007;26:7508–16.

21. Moeller BJ, Cao Y, Li CY, Dewhirst MW. Radiation activates HIF-1 to regulate vascular radiosensitivity in tumors: role of reoxygenation, free radicals, and stress granules. Cancer Cell 2004;5:429–41.

22. Moeller BJ, Dreher MR, Rabbani ZN, et al. Pleiotropic effects of HIF-1 blockade on tumor radiosensitivity. Cancer Cell 2005;8:99–110.

23. Harada H, Hiraoka M, Kizaka-Kondoh S. Antitumor effect of TAT-ODD-caspase-3 fusion protein specifically stabilized and activated in hypoxic tumor cells. Cancer Res 2002;62: 2013–8.

24. Harada H, Kizaka-Kondoh S, Hiraoka M. Optical imaging of tumor hypoxia and evaluation of efficacy of a hypoxia-targeting drug in living animals. Mol Imaging 2005;4:182–93.

25. Harada H, Kizaka-Kondoh S, Hiraoka M. Mechanism of hypoxia-specific cytotoxicity of procaspase-3 fused with a VHL-mediated protein destruction motif of HIF-1α containing Pro564. FEBS Lett 2006;580:5718–22.

26. Hiraga T, Kizaka-Kondoh S, Hirota K, Hiraoka M, Yoneda T. Hypoxia and hypoxia-inducible factor-1 expression enhance osteolytic bone metastases of breast cancer. Cancer Res 2007;67: 4157–63.

27. Inoue M, Mukai M, Hamanaka Y, Tatsuta M, Hiraoka M, Kizaka-Kondoh S. Targeting hypoxic cancer cells with a protein prodrug is effective in experimental malignant ascites. Int J Oncol 2004; 25:713–20.

28. Kizaka-Kondoh S, Inoue M, Harada H, Hiraoka M. Tumor hypoxia: a target for selective cancer therapy. Cancer Sci 2003;94:1021–8.

29. Schwarze SR, Ho A, Vocero-Akbani A, Dowdy SF. *In vivo* protein transduction: delivery of a biologically active protein into the mouse. Science 1999;285:1569–72.

30. Chen C, Okayama H. High-efficiency transformation of mammalian cells by plasmid DNA. Mol Cell Biol 1987;7:2745–52.

31. Onn A, Isobe T, Itasaka S, et al. Development of an orthotopic model to study the biology and therapy of primary human lung cancer in nude mice. Clin Cancer Res 2003;9:5532–9.

32. Semenza GL. Evaluation of HIF-1 inhibitors as anticancer agents. Drug Discov Today 2007;12: 853–9.

33. Storey KB, Storey JM. Metabolic rate depression in animals: transcriptional and translational controls. Biol Rev Camb Philos Soc 2004;79:207–33.

34. Shah K, Tung CH, Breakefield XO, Weissleder R. *In vivo* imaging of S-TRAIL-mediated tumor regression and apoptosis. Mol Ther 2005;11: 926–31.

35. Forsythe JA, Jiang BH, Iyer NV, et al. Activation of vascular endothelial growth factor gene transcription by hypoxia-inducible factor 1. Mol Cell Biol 1996;6:4604–13.

36. Büchler P, Reber HA, Büchler M, et al. Hypoxia-inducible factor 1 regulates vascular endothelial growth factor expression in human pancreatic cancer. Pancreas 2003;26:56–64.

37. Morris MC, Depollier J, Mery J, Heitz F, Divita G. A peptide carrier for the delivery of biologically active proteins into mammalian cells. Nat Biotechnol 2001;19:1173–6.

38. Zhao Q, Du J, Gu H, et al. Effects of YC-1 on hypoxia-inducible factor 1-driven transcription activity, cell proliferative vitality, and apoptosis in hypoxic human pancreatic cancer cells. Pancreas 2007;34:242–7.

Clinical Cancer Research

Selective Killing of Hypoxia-Inducible Factor-1–Active Cells Improves Survival in a Mouse Model of Invasive and Metastatic Pancreatic Cancer

Shinae Kizaka-Kondoh, Satoshi Itasaka, Lihua Zeng, et al.

Clin Cancer Res 2009;15:3433-3441.